Egyptian Journal of Pure and Applied Science

Reactions of 2'-hydroxy methoxylated chalcone with group 6 and 8 metal carbonyl complexes under sunlight irradiation: Synthesis, characterization, spectroscopic investigation and biological activities

Mostafa M.H. Khalil, Ramadan M. Ramadan, Mounir A.I. Salem*, Magda I. Marzouk,
Mohamed S. Moftah

Department of Chemistry, Faculty of Science, Ain Shams University, Abbassia, 11566, Cairo. Egypt.

ARTICLE INFO

ABSTRACT

Sunlight irradiation of the reactions of either $[M(CO)_6]$, M=Cr, Mo and W or $[M_3(CO)_{12}]$, M = Ru or Os with 1-(2'-Hydroxyphenyl)-3-(3``,4``-dimethoxyphenyl)-2-propen-1-one, **1**, in benzene were investigated. Three dinuclear complexes with molecular formulas $[Cr_2O_2(ChO)_2]$, **2**, $[Mo_2O_4(ChO)_2]$, **3**, $[W_2O_4(ChO)_2]$, **4**, were isolated from the reactions with **1**. The corresponding reactions of **1** with group 8 cluster complexes produced the complexes, $[Ru_3(CO)_{10}(ChO)]$, **5**, and $[Os_3(CO)_{10}(ChOH)]$, **6**. All complexes were characterised by elemental analysis, infrared, ^{1}H-NMR, (^{13}C-NMR for **1**), mass and ESR spectroscopy. The UV–vis spectra of the complexes showed visible bands due to either ligand-to-metal or metal-to-ligand charge transfer. Thermal properties of the complexes were investigated by TG thermogravimetric technique. The synthesized **1** (ligand) and its complexes were screened for their antibacterial activity against two gram positive bacteria, two gram negative bacteria and fungi *candida albicans*. The activity was compared with Amikacin as standard.

Introduction

Chalcones and their analogues are well known for having variable germicidal[1], bactericidal[2], fungicidal[3], anti-inflamatory[4], antihyperglycemic[5] and carcenogenic activity[6-8].

A wide range of pharmacological activities have been identified for various chalcones. These include antioxidants, antitumers[9], antimalarial[10] and anticancer activities[11]. Cytotoxic effects of antioxidant flavonoids (including chalcones) are associated with their pro-oxidant effects[12]. The antioxidant properties of chalcones are known to be influenced to a great extent by the two aryl structures, that is, the substitutions on two aryl rings of chalcone molecule and their substitution patterns. Especially, the hydroxyl substituent is one of the key groups to enhance greatly the antioxidant activity of chalcone mainly due to its easy conversion to phenoxy radicals through the hydrogen atom transfer mechanism[13].

Synthesis of some complexes of chalcones and their bio-

* Corresponding author.
  E-mail address: Salemmai1947@yahoo.com.

logical activities are available in literature; for example chalcone-tellurium complexes[14], are active in the inhibition of E. Coli. Also, Ru(II)/Ru(III) polypyridyl complexes containing 2,6-(2'-benzimidazolyl)-pyridine /chalcone as co-ligand[15] have found to exhibit anti-HIV and cytotoxic activities. 2'-hydroxychalcone was the most effective in enzyme activities and gene expressions[16]. Metal chelates of some divalent transition metal ions (Co(II), Ni(II), Cu(II), Pt(II) and Pd(II)) of 2'-hydroxychalcone standout as distinct class of o-hydroxycarbonyl compounds with low spin square-planar configuration, which do not easily form adduct, because of the extensive conjuagation[17,18]. This is in contrast to metal (II) chelate of β-diketones, salicyaldehyde, o-hydroxyarylketone and o-hydroxy-crotonophenone, which have high-spin octahedral configuration[19]. 2'-Hydroxychalconate complexes of ruthenium (II) containing triphenylphosphine or triphenylarsine have been found to show significant catalytic oxidation and biological activities[20,21]. Recently, a synthetic precursor cis-$[Ru^{II}Cl_2(dmso)_4]$ is complexed separately with 3-(4-benzyloxyphenyl)-1-

(2-hydroxylphenyl)-prop-2-en-1-one (L^1H) and 2-(4-benzyloxyphenyl)-3hydroxy-chromen-4-one (L^2H). The resulting complexes are assigned the composition *fac*-[RuCl(S-dmso)$_3$(L^1)] and *fac*-[RuCl(S-dmso)$_3$(L^2)]. The X-ray diffraction analysis showed that the complexes self-associate through non-covalent interactions and provide 1D and 2D supramolecular structures. These complexes are assayed for their cytotoxicity studies on Dalton Lymphoma cell lines[22].

There were no previous studies documented according to our knowledge on the reaction of 2-hydroxychalcone or its derivative with metal carbonyls in the literature. Only few examples on the preparation of the compounds [Fe(Ch)(CO)$_3$], ch = chalcone[23] by thermal procedure and [Fe(Ch)(CO)$_2$PPh$_3$] by irradiation of a solution of tetracarbonyltriphenylphosphineiron with chalcone[24]. In this paper, synthesis of the ligand, (2'-hydroxyphenyl)-3-(3'-4'-dimethoxyphenyl)prpen-1-one, **1**, and its photochemical reactions with metal carbonyl complexes of groups 6 and 8 under sunlight irradiation are described.

Experimental procedures

Chemicals

2-Hydroxyacetophenones, 3,4-dimethoxybenzaldehyde, M(CO)$_6$, M= Cr, Mo or W and M$_3$(CO)$_{12}$; M = Ru or Os were purchased from Aldrich. All solvents were of analytical grade and were purified by distillation before use.

Instrumentation

Infrared measurements were carried out on a Unicam-Mattson 1000 FTIR spectrometer using KBr pellets. Nuclear magnetic resonance measurements were performed on a Spectrospin-Bruker AC 200 MHz spectrometer. Samples were dissolved in DMSO, d$_6$ using TMS as internal reference. UV-vis measurements were carried out on a Unicam UV2-300 spectrophotometer with 10 mm quartz cell. Magnetic susceptibility of the paramagnetic chromium complex in the solid state (Gouy method) was recorded on a Sherwood magnetic susceptibility balance. Diamagnetic correction was made by Pascal's constant and Hg[Co(SCN)$_4$] was used as a calibrant. Mass spectra of the solid complexes (70 eV, EI) were carried out on a Shimadzu Qp-2010 Plus spectrometer (charts 1 to 4). Thermogravimetric analyses were carried out under nitrogen atmosphere with a heating rate of 10°C/min using a Schimadzu DT-50 thermal analyzer. Elemental analyses were performed on a Perkin–Elmer 2400 CHN elemental analyzer. Tables 1 and 4 give the elemental analysis and mass spectrometry data for the complexes.

Synthesis of 1-(2'-Hydroxyphenyl)-3-(3``,4``-dimethoxyphenyl)-2-propen-1-one (ChOH), 1

A mixture of 2-hydroxyacetophenones (16.33 g, 0.12 mole) and 3,4-dimethoxybenzaldehyde (19.92 g, 0.12 mole) in a round bottom glass (pyrix) flask (250 mL), in pure ethanol 96% (100 mL) are stirred for 30 minutes at room temperature and then 15 ml of an aqueous solution of sodium hydroxide (0.2M) was added to it. The mixtu-

re was stirred for 4h and kept overnight at room temperature. The reaction mixture was poured into crushed ice and acidified with dilute hydrochloric acid (18 mL, 2N). The chalcone derivative precipitates out as solid then filtered off, washed with water several times and dried at room temperature using a water pump to yield **1**.

General procedure for the preparation of the complexes of some group-6 elements

a. [Cr$_2$O$_2$ (ChO)$_2$], 2

A mixture of Cr(CO)$_6$ (0.1g, 0.45 mmol) and 3-(3',4'-dimethoxyphenyl)-1-(2-hydroxyphenyl)prop-2-en-one (0.13g, 0.45 mmol) dissolved in 25 mL benzene in glass (pyrix) round bottom flask (250 mL) and left in sunlight for 3 days in summer time ($850 – 1000$ w/m^2). The color of the solution changed from yellow to brown with formation of brown precipitate. The solvent was evaporated under reduced pressure using rotatory evaporator to give a solid residue which was washed several times with boiling petroleum ether (60/80) filtered off and dried to give **2**.

b. [Mo$_2$O$_4$(ChO)$_2$], 3

A similar method as used for synthesis of [Cr$_2$O$_2$ (ChO)$_2$] was employed. The reaction time was (2 days).

c. [W$_2$O$_4$(ChO)$_2$], 4

A similar method as used for synthesis of [Cr$_2$O$_2$ (ChO)$_2$] was employed. The reaction time was (2 days).

General procedure for the preparation of the complexes of some group-8 elements

d. [Ru$_3$(CO)$_{10}$(ChO)], 5

A mixture of Ru$_3$(CO)$_{12}$ (0.15g, 0.23mmol) and ChOH (0.06g, 0.23 mmol) were mixed in *ca* 30 mL benzene. The mixture was left under sun irradiation for 6 days during which a brown precipitate was formed. The solvent was removed under reduced pressure using a rotatory evaporator and the solid residue was washed several times by hot petroleum ether (60-80) as to give dark brown amorphous solid.

e. [Os$_3$(CO)$_{10}$(ChOH)], 6

A similar method for synthesis of [Ru$_3$(CO)$_{10}$(ChO)] was employed. The reaction time was (8 days).

Antimicrobial activity

The ChOH ligand and its complexes were screened for their antibacterial activity using the agar diffusion technique[25]. A 2.5mg/mL solution in DMF was used. The tested organisms were two gram positive bacteria *viz., Bacillus subtilis, Staphylococcus aureus, E-Coli* and two gram negative bacteria *viz., Escherichia coli , Pseudomonas aerogenasa* and unicellular fungi as *candida albicans.* The bacteria and fungi were maintained on nutrient agar medium and Czapeks Dox agar medium, respectively. The agar media were inoculated with different test microorganisms. After 24h of incubation at 30°C for bacteria and 48 h of incubation at 28 ^{0}C for fungi, the diameter of inhibition zone (mm) was measured. A reference standard for both gram positive and gram negative bacteria was made by dissol-

ving accurately weighed quantity of Amikacin (0.0025 gm) in sterile distilled water (1 mL), separately.

X-ray data collection and structure refinement (Tables 2 and 3)

The X-ray diffraction data for (ChOH) were collected at room temperature on a maXus (Bruker Nonius, Delft & Mac Science, Japan) using MoKa radiation. A standard reflection was monitored every 100 reflections, during the data collection process, without significant variations. The structure was solved with SIR92[26] and the refinements were carried out with maXus[27]. For the present structure most hydrogen atoms were found in a final ΔF map, the remaining hydrogen atoms were put in their theoretical positions and refined automatically. Cambridge Crystallographic Data Centre CCDC-802359. The molecular structure of 2-hydroxychalcone is shown in Figure 1. Crystallographic data for the structure are given in Table 2[28], while the selected bond length and angles are given in Table 3.

1
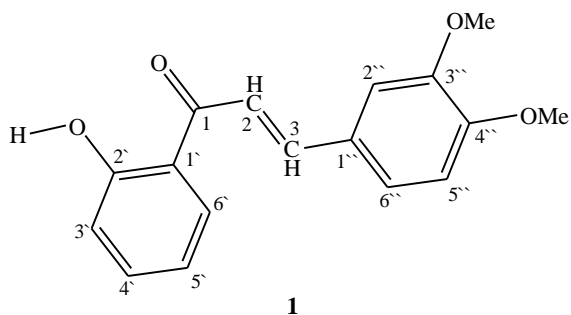
Results and Discussion

Infrared and NMR studies of the ligand (Table 4)

The infrared spectrum of the ChOH ligand (Table 4) exhibited a strong stretching frequency band for the carbonyl group at 1725 cm^{-1} and two strong bands at 1573 and 1631 cm^{-1} due to υ(C=C). Furthermore, the IR spectrum displayed a broad weak band at 3403 cm^{-1} due to the stretching frequencies of the OH group. Moreover, the bands at 1267 and 1150 cm^{-1} assigned to the O-ph and O-CH$_3$, respectively. The ^{1}H NMR spectrum of **1** in deuterated DMSO showed a broad singlet signal at 12.82 ppm due to OH forming intermolecular hydrogen bonding with the carbonyl group. Also, the ^{1}H NMR spectrum exhibit doublet signal at 8.3 ppm due to (Ar-CH=CH-, J = 12.3 Hz), as well as multiplets in the range 6.90-7.8 ppm due to the phenyl protons.

Infrared and NMR studies of 1 complexes (Table 4)

The photochemical irradiation by sunlight of the reaction of [M(CO)$_6$], M= Cr, Mo and W, with 1-(2'-Hydroxyphenyl)-3-(3``,4``-trimethoxyphenyl)-2-propen-1-one (ChOH) resulted in the formation of different complexes depending on the metal type and the reaction time. While the reaction with [Cr(CO)$_6$] gave the binuclear complex [Cr$_2$O$_2$(ChO)$_2$] **2**, with the metal atom in +3 formal oxidation state, molybdenum and tungsten hexacarbonyls gave the oxo derivatives

[Mo$_2$O$_4$(ChO)$_2$] **3**, and [W$_2$O$_4$(ChO)$_2$] **4**, with +5 formal oxidation states for molybdenum and tungsten, respectively. On the other hand, sunlight irradiation of M$_3$(CO)$_{12}$, M = Ru and/or Os resulted in the formation of cluster complexes Ru$_3$(CO)$_{10}$(ChO), **5** with Ru atom in +1 formal oxidation state and M$_3$(CO)$_{10}$(ChOH), **6** where M = Os in zero oxidation state. It is expected that the formation of complexes were proceeded via the M(CO)$_5$ intermediate through M-CO bond dissociation[29-33]. These 16-electron containing M(CO)$_5$ fragments react avidly with either the ligand alone to give metal derivative (as with group 8 products)[34] or with the ligand and oxygen to give oxocomplexes [as with group 6 products). The source of oxygen in the oxo complexes could be originated from the dissolved oxygen in the used solvent. It is well established that both molybdenum and tungsten have higher affinity to react with oxygen[35,36]. Compared with the IR spectra of **1**, the absorption bands of complexes exhibited downward shifts (7-18 cm^{-1}) for the C=O group of the ligand indicating that coordination occurred via oxygen atom of the carbonyl oxygen group. Infrared spectrum of the complexes indicated that the carbonyl group is perturbed only slightly by coordination to metal. A change in metal affects υ_{CO} and υ_{MO} and other vibrations. For Cr, Mo and W complexes, new bands in the region of 500–800 cm^{-1} were assigned to stretching vibrations of υ(M–O). The mass spectrum of the three complexes showed a molecular ion peak at *m/z* corresponding to the parent peak (Table 4).
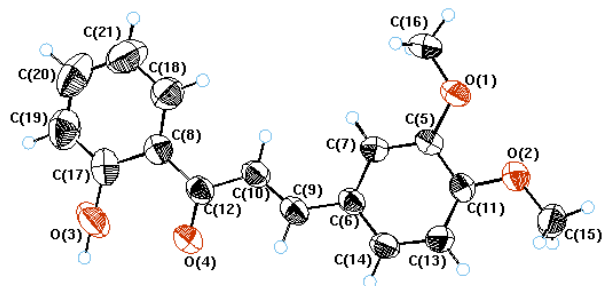

Fig. 1: Anisotropic ellipsoid representation of **1**. The ellipsoids are drawn at 50% probability level.

The infrared spectrum of the chromium complex **2**, displayed the characteristic bands of ChOH with the appropriate shifts due to complex formation (Table 4). The disappearance of OH frequency in the complex suggested that the chromium coordinated to the ligand through oxidative addition of OH group with loss of a proton. The infrared spectrum of the complex also exhibited two non-ligand bands at 575 and 672 cm^{-1} due to Cr–O and bridged Cr-O-Cr bonds, respectively[37]. Therefore, it can be suggested that ChOH ligand probably coordinated to chromium atom through phenolic oxygen and carbonyl oxygen and acting as a bidentate ligand. From the elemental analysis (Table 1) and spectroscopic data, it can be concluded that the binuclear chromium complex has tetrahedral configuration with each chromium coordinated to one

ligand and bonded to two bridged oxygen atoms as shown in Scheme 1. This structural arrangement would give a chromium species with +3 (d^3) formal oxidation state. Measurements of the magnetic susceptibility of solid $Cr_2O_2(chO)_2$ at 298°K (Gouy method) gave an effective magnetic moment of (2.50 B.M). The observed μ_{eff} indicated that the corresponding value for each chromium species (1.25 BM) was less than the spin–only momentum of one unpaired electron which was not expected for a d^3 metal center with three unpaired electrons. This could be retained to the existence of strong antiferromagnetic coupling between the two metal centers. However, the tetraheral arrangements was observed for $Cr_2O_2(isat)_2$, isat = isatin[34]. The low effective magnetic moments was observed for many chromium complexes[34,38]. Furthermore, the ESR spectra of the complex recorded as polycrystalline sample, Fig 2, gives one broad isotropic signal centered approximately at around the free electron $<g>$ value of 1.9839. The broadening of the spectra is due to spin relaxation[39]. Tetrahedral chromium (III) complexes are rare, found only with sterically-demanding ligands[35]. Since a single crystal of the complex was difficult to obtain, we cannot exclude the possibility that complex (**2**) exists as a tetramer with cubane Cr_4O_4 arrangement.

The sun irradiation of a mixture of $[M(CO)_6]$; M =Mo or W and ChOH in benzene produced the binuclear oxo-complexes $[M_2O_4(ChO)_2]$, M = Mo or W. The infrared spectrum of the two complexes displayed similar features suggesting that the complexes may have similar structures, Table 4. Both complexes exhibited bands in the range of 968-976 cm^{-1} characteristic to Mo=O and W=O bonds. Furthermore, non-ligand bands at 757 and 760 cm^{-1} for molybdenum and tungsten complexes, attributed to M-O-M bonds in the molybdenum and tungsten complexes, respectively. Such arrangement lead to the formation of paramagnetic oxo Mo(V) and W(V), d^1 complexes. Upon complex formation, the proton of the coordinated hydroxyl group was lost, probably *via* an oxidative addition which would result in the formation of a molybdenum (V) and tungsten (V) species.

Magnetic susceptibility measurement of the molybdenum and tungsten complexes at room temperature gave an effective magnetic moment of 2.50 and 1.12 B.M, respectively. The ESR spectra of the molybdenum and tungsten complexes recorded as polycrystalline sample at room temperature are shown in Figure 3. The ESR signal of W(V) is quite similar to that of Mo(V) in its line shape, thus supporting the suggestion that the two metal ions are present in the same environment in the two complexes. The W(V) signal has g values (g$_{||}$ = 1.91658, g$_\perp$ =1.92795) lower than those of the Mo(V) signal (g$_{||}$ =1.93587, g$_\perp$ =1.94328).

The W(V) is 5d^1 and S=1/2. From the positive sign of the spin orbit coupling constant with less than half-field basic theory predict the g-values to be less than that of the free electron value, g$_e$ = 2.0023. Experimental value

for W(V) are typically in the range of 1.9-1.7[40] and the deviation from g$_e$ as well as the overall g-anisotropy are somewhat more pronounced than in molybdenum. Natural W consists of five isotopes, only one of which has nuclear spin: ^{183}W occurs in a natural abundance of 14.4% and has a nuclear spin I=1/2. The isotope is frequently detectable in the S=1/2 spectra of W(V) in the form of small satellite lines with circa 7% relative intensity.

Many oxo molybdenum and tungsten complexes were previously reported. For example, interaction of bis-(salicylaldehyde)etylenediimine (salenH$_2$) and 2-hydroxyacetophenoneethylene-diimine (hapenH$_2$) with Mo(CO)$_6$ in THF under atmospheric pressure gave Mo(O)(salen) and Mo(O)(hapen) with the metal atom in +4 oxidation state[37,41]. Also, reactions of the Schiff base salicylideneimine-2-anisole (salanH) with M(CO)$_6$, M=Mo or W, gave the dinuclear oxo complex $M_2O_4(salan)_2$[42].
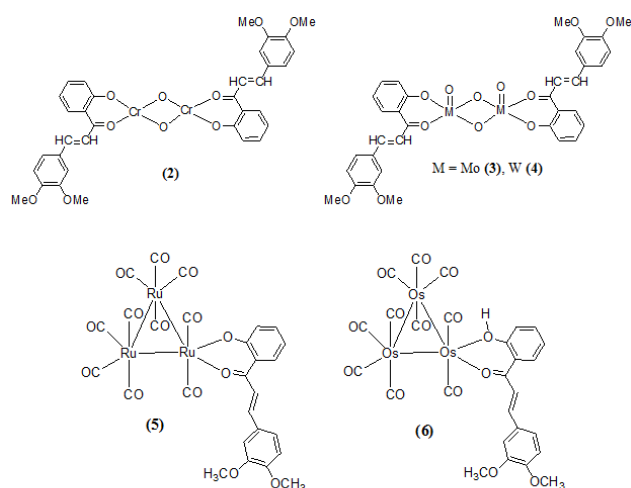
Scheme 1

Sun irradiation of group 8 metal carbonyls in the presence of **1** (ChOH) results in the formation of $Ru_3(CO)_{10}(ChO)$ **5** and $Os_3(CO)_{10}(ChOH)$ **6**, which are isolated and characterized by elemental analysis, FTIR, ^{1}H-NMR, and mass spectra.

The FTIR spectrum of the ruthenium complex exhibits three prominent bands at 2046s, 1972s, 1935s in the CO stretching vibrational region. On the other hand, osmium complex exhibit three bands at 2126, 2037 and 1958 cm^{-1} due to terminal carbonyls of cluster complex. ^{1}H NMR of the osmium complex showed signals similar to that of the ligand with shift of OH signal from 12.82 of the ligand to 12.75 ppm . On the other hand, the ^{1}H-NMR spectra of the ruthenium complex showed no signal due to the paramagnetic characteristics of the ruthenium complex. The absorption due to νO–H was not observed in the infrared spectra of the ruthenium complex in the region 3400–3600 cm^{-1} suggesting the deprotonation of the ligand prior to coordination. Magnetic measurement of the complex at 298K gave an effective magnetic moment μeff of 1.70 BM which is close to the spin-only moment of an unpaired electron (1.73 BM). According to the spectroscopic data available, the suggested struct-

ures of the ruthenium **5** and osmium **6** complexes are as shown in Scheme 1.

UV-vis studies

Figure 5 shows the absorption spectra of ChOH and its complexes in DMSO. The absorption band of the ChOH in DMSO exhibited a band at 400 nm corresponded to n–π* electronic transition. This band was hypsochomically shifted upon complexation. In addition, a new broad band appeared around 500 nm upon complex formation that can be assigned for ligand to metal charge transfer in chromium and molybdenum complexes. For osmium and complexes, the band at 470 nm could be assigned as metal-to-ligand charge transfer.
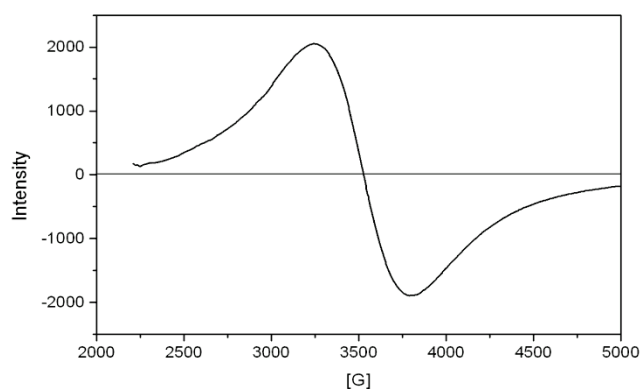
Fig. 2: The X-band ESR spectrum of polycrystalline [$Cr_2O_2(Ch)_2$] at room temperature.
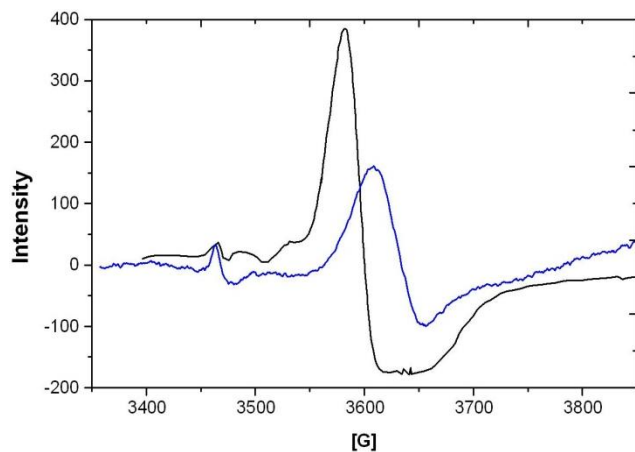
Fig. 3: The X-band ESR spectrum of polycrystalline (——) [$Mo_2O_4(Ch)_2$] and (——) [$W_2O_4(Ch)_2$] at room temperature.

Thermogravimetric analysis

In order to get more information about the structure of the complexes and their thermal stability, the thermal studies of the complexes were carried out using thermogravimetry (TG) technique. The data of thermal study of the complexes are presented in Table 5. The most stable complexes were the molybdenum (V) and tungsten (V) complexes. The [$Ru_3(CO)_{10}$(ChO) and [$Os_3(CO)_{10}$(ChOH) complexes exhibited similar behavior of losing the 10 CO groups and one ligand but the osmium complex showed no residue.

Antimicrobial activity

The synthesized ChOH ligand and its complexes were screened for their antibacterial activity against two gram positive bacteria, two gram negative bacteria and fungi *Candida albicans*. The inhibition zone produced by each compound was measured in mm. The results of antibacterial studies are given in Table 6. All the tested complexes showed antimicrobial activity and the activity of the complexes is higher than that of the ligand against *E. Coli*. Furthermore, the Minimum Inhibitory Concentration (M.I.C) of ChOH and its complexes against microorganisms are shown in Table 7.

The tested compounds (**2**, **3**, **4**, **5**, **6**) showed antimicrobial activity against 2 Gram positive organism namely *Bacillus subtillus* and *Staphylococcus aureus* and 2 Gram –ve organism namely *Psendomonas aeruginosa* and *E. coli*, in addition to the yeast fungi *Candida albicans*. On the other hand, *Aspergillus niger* was not inhibited by any of the tested compounds.

The maximum antimicrobial activity against *Bacillus subtillus*, *Staphylococcus aureus*, *Psendomonas aeruginosa*, *E. coli* and *Candida albicans* was detected with compounds **1, 2, 3, 4, 5** and **6** respectively.

All tested compounds showed lower antimicrobial activities against the tested organism as compared to the standard antibiotic (Amikacin).
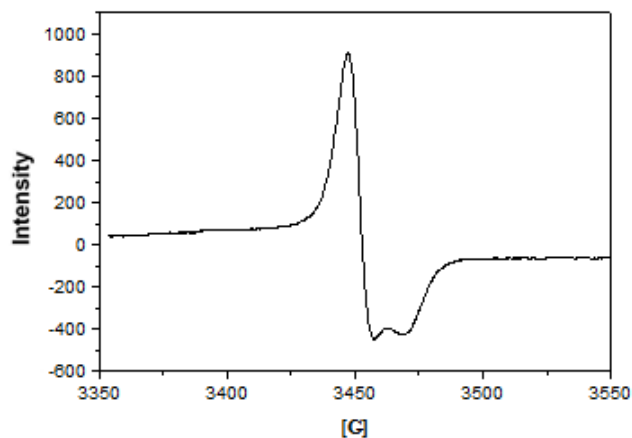

Fig. 4: The X-band ESR spectrum of polycrystalline [$Ru_3(CO)_{10}$(Ch-H)].

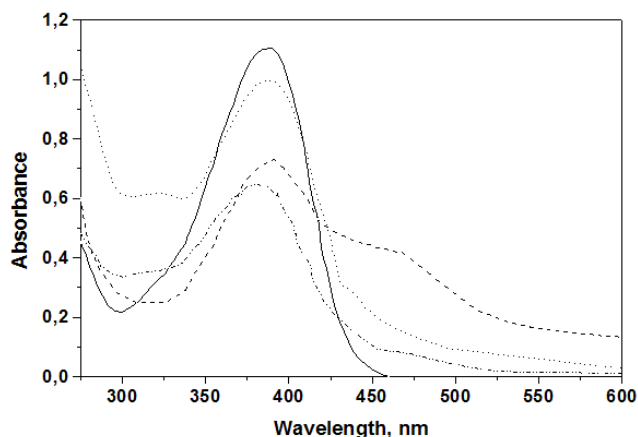**Fig. 5:** UV-Vis spectra of ChOH and its complexes in DMSO: ChOH (——),[Cr_2O_2(ChO)$_2$ (----), [Mo_2O_4(ChO)$_2$] (…..) and [$Os_3(CO)_{10}$(ChOH)] (-··-).

The MIC (minimum inhibitory concentration): The lowest MIC against *Bacillus subtillus* was found to be 156 μg/L for **2** and **6**. For *S. aureus*, all compounds MIC of 312, for *E. Coli* compound **4** only showed MIC of 312 while all other tested compounds had MIC of 623. For *P. aeruginosa* compound **1** and **6** had the same MIC of 312. Finally, the MIC against *Candida albicans* for compounds **4** and **5** was 312 while compounds **6** showed MIC of 625.

Conclusion

Sunlight irradiation was found to be an excellent source of energy for preparing new interesting species from the metal carbonyls. An oxo-bridged binuclear derivative $[CrO(ChO)_2]$ was isolated from the interaction of 2'-hydroxychlcone (ChOH) with $[Cr(CO)_6]$. On the other hand, binuclear derivatives $[M_2O_4(ChO)_2]$ with terminal and bridged oxygens were obtained from the corresponding reactions of molybdenum and tungsten carbonyls. Furthermore, cluster complexes of group 8 metal carbonyls were isolated under sunlight irradiation where only two CO groups were substituted by the ligand. It was found that the type of bonding of ChOH is dependent on the metal type.

Table 1: Physical characterization of compounds.

Compound No.	m.p.,°C (Colour)	Solvent (% yield)	MF (M.wt.)	Elemental analysis Calcd/Found	
				%C	**%H**
1	110-112 Yellow	Pe.ether 60/80 (94%)	$C_{17}H_{16}O_4$ (284.311)	71.82 72.13	5.67 5.72
2	> 260 Brown	Ethanol (84%)	$C_{34}H_{30}O_{10}Cr_2$ (702.598)	58.12 57.86	4.30 4.71
3	> 260 Brown	Ethanol (77%)	$C_{34}H_{30}O_{12}Mo_2$ (822.481)	49.65 51.24	3.67 3.93
4	> 260 Brown	Ethanol (79%)	$C_{34}H_{30}O_{12}W_2$ (998.304)	40.90 41.06	3.02 3.18
5	> 260 Brown	Ethanol (83%)	$C_{27}H_{15}O_{14}Ru_3$ (866.617)	37.42 37.29	1.74 1.78
6	> 260 Brown	Ethanol (75%)	$C_{27}H_{16}O_{14}Os_3$ (1135.105)	28.56 28.42	1.42 1.60

Table 2. Spectroscopic data for mdba and its complexes.

Crystal parameters

Empirical formula	$C_{17}H_{16}O_4$
M.wt.	284.311
Space group	$P2_1/c$ Monoclinic
a / Å	14.2530 (7)Å
b / Å	8.0238 (3)Å
c / Å	13.6115 (5)Å
α / deg	90.00
β / deg	110.052(5)
γ / deg	90.00
V / Å³	1462.29 (11)Å³
Z	4
T / K	298
ρ_{calc} / g cm⁻³	1.418
θ	2.910—27.485 °
μ / mm⁻¹	0.09 mm⁻¹
R^a	0.038
R_w^b	0.055
(MoKα)/ Å	0.71073

Table 3. Important bond lengths of **1**

O1—C5	1.362 (3)
O1—C16	1.403 (3)
O2—C11	1.367 (3)
O2—C15	1.426 (3)
O3—C17	1.338 (3)
O4—C12	1.239 (3)
C5—C7	1.380 (3)
C5—C11	1.400 (3)
C6—C7	1.405 (3)
C6—C9	1.456 (3)
C6—C14	1.382 (3)
C8—C12	1.460 (4)
C8—C17	1.420 (4)
C8—C18	1.400 (4)
C9—C10	1.331 (3)
C10—C12	1.464 (4)
C11—C13	1.375 (3)
C13—C14	1.388 (4)
C17—C19	1.371 (4)
C18—C21	1.368 (4)
C19—C20	1.358 (5)
C20—C21	1.388 (5)

Table 4. Physical characterization of compounds

Comp. No.	IR KBr, ν_{max} (cm^{-1})	^{1}H-NMR δ (ppm)	^{13}C-NMR δ (ppm)	MS: m/z (%) relevant fragments
1	ν_{OH} at 3403, $\nu_{C=O}$ at 1725 and $\nu_{C=C}$ at 1631 cm^{-1}	12.8 (s, H, OH), 8.3 (d, 2H, CH=CH, J = 12.3 Hz), 7 (m, 7H, Ar), 3.95 (s, 6H, 2OCH$_3$).	C$_1$ (193.54), C$_{4``}$ (162.24), C$_{3``}$ (151.67), C$_{2`}$ (149.04), C$_{2``}$ (145.56), C$_{6``}$(136.04), C$_{3`}$ (131.7), C$_{6`}$ (129.7), C$_{5`}$ (128.1), C$_{1`}$ (120.36), C$_3$ (118.84), C$_2$ (117.67), C$_{7``}$ (55.68), C$_{8``}$ (5.42)	284 (22.1), 268 (19.4), 254 (9.10), 224 (4.4), 209 (10.6), 192 (0), 164 (35.4), 147 (17.7), 138 (14.2), 133 (10.6), 122 (4.4), 121 (63.7), 105 (23.9), 103 (7.1), 93 (29.2), 92 (13.3), 77 (52.2), 76 (27.4), 66 (100), 64 (19.5), 62 (23.91), 53 (50.4). c.f (Chart 1)
2	$\nu_{OH\ inter\ H-bond}$ 3406, $\nu_{C=O}$ at 1718, $\nu_{C=C}$ 1623, ν_{Cr-O} at 575 and $\nu_{bridged\ Cr-O-Cr}$ at 762 cm^{-1}	8.3 (d, 2H, CH=CH, J = 15.3 Hz), 7.8 (m, 7H, Ar), 3.89 (s, 6H, (2OCH$_3$).	-	[M + 2] 704.4 (9.42), 672.7 (5.33), 582 (6.88), 570 (6.17), 532 (6.69), 514.80 (4.19), 504 (7.09), 484.6 (7.06), 486.75 (6.19), 366.4 (9.00), 364.55 (8.54), 352.7 (4.09), 305 (10.40), 291.6 (9.15), 285.05 (14.91), 284.10 (100), 283.15 (28.52), [Lig – OH] 267.30 (9.15), [Lig – OCH$_3$] 253.05 (15.25), [Lig – 2OCH$_3$ + H] 233 (13.55), 223 (13.55), [Lig – 2OCH$_3$] 221.75 (4.33), 220.80 (14.44), 151.05 (64.97), 148.15 (10.19), 132.35 (13.88), 130.10 (5.37), 122.10 (11.98), 121.15 (28.49), 105.10 (14.02), 77 (24.56), 66.15 (19.90), 64.20 (12.11), 56 (25.3), 52 (20.36). c.f (Chart 2)
3	$\nu_{inter\ H-bond}$ 3429, $\nu_{C=O}$ at 1725, $\nu_{C=C}$ 1627, ν_{Mo-O} at 568 and $\nu_{bridged\ Mo-O-Mo}$ at757 and $\nu_{Mo=O}$ at 968 cm^{-1}	8.25 (d, 2H, CH=CH, J = 6 Hz), 7.40 (m, 7H, Ar), 3.86 (s, 6H, 2OCH$_3$).	-	822.48 (0), [M – OCH$_3$ + 3H] 794.7 (13.25), 284.7 (16.61), 283.65 (30.07), [Lig – OH + H] 268.80 (11.83), [Lig – OCH$_3$] 253 (12.95), [Lig – 2OCH$_3$] 222.80 (16.61), 191.48 (12.51), 174.8 (12.15), 160 (14.51), 151.05 (100), 122.9 (13.51), 120.9 (62.57), 105.10 (18.45), 103.10 (14.20), 93.10 (19.45), 77 (38.59), 66 (34.12), 64 (23.87), 56 (28.71), 52.70 (16.35). c.f (Chart 3).
4	$\nu_{inter\ H-bond}$ 3428, $\nu_{C=O}$ at 1725, $\nu_{C=C}$ at 1612, ν_{W-O} at 664 and $\nu_{bridged\ W-O-W}$ at760 and $\nu_{W=O}$ at 976 cm^{-1}	8.8 (d, 2H, CH=CH, J = 10.5 Hz), 7.57 (m, 7H, ArH), 3.70 (s, 6H, 2OCH$_3$).	-	998.30 (0), 284.4 (15.86), 283.40 (35.82), [Lig – OH] 267 (26.94), [Lig – OCH$_3$] 253 (35.94), [Lig – 2OCH$_3$] 222 (30.15), 191.45 (34.12), 174.20 (25.71), 161 (31.03), 151.50 (39.68), 123.05 (53.45), 121.9 (39.08), 105 (53.68), 102.95 (54.37), 93.30 (36.28), 78.75 (49), 66.95 (40.02), 63.80 (80.99), 56 (74.9), 51.90 (47.7). c.f (Chart 3).
5	$\nu_{inter\ H-bond}$ 3409, $\nu_{C=O}$ at 1718, $\nu_{C=C}$ at 1558, ν_{RuCO} at 2046, 1972, 1935 cm^{-1}	7.59 (d, 2H, CH=CH, J = 8.7 Hz), 7.30 (m, 7H, Ar), 3.80 (s, 6H, 2OCH$_3$).	-	866.617 (0), [M – 4] 862.9 (10.99), 797.90 (12.21), 682.90 (16.03), 533.90 (10.93), [Lig – H$_2$O] 266 (12.95), 265.90 (12.9), 251.90 (10.67), 209 (10.6), 190 (0), 164 (35.4), 156.90 (11.15), 154.90 (12.10), 152.90 (11.84), 124.90 (14.65), 121.90 (12.95), 106.10 (12.26), 93 (29.2), 82.10 (11.36), 93 (29.2), 92.10 (27.28), 90.10 (15.82), 82.10 (11.36), 83.10 (14.12), 79.10 (13.54), 76 (17.4), 73.10 (16.35), 66 (81.43), 64.10 (21.97), 62 (29.99), 56.10 (100), 55.15 (77.39), 53 (16.45), 51 (20.17). c.f (Chart 4).
6	$\nu_{inter\ H-bond}$ 3422, $\nu_{C=O}$ at 1703, $\nu_{C=C}$ at 1559, $\nu_{OsCO\ terminal\ carbonyl}$ at 2126, 2037, 1959 cm^{-1}	12.75 (s, H, OH), 8.30 (d, 2H, CH=CH, J = 6.6 Hz), 7.41 (m, 7H, Ar), 3.83 (s, 6H, 2OCH$_3$)	-	989.60 (49.23), 954.95 (47.09%), 944.60 (46.36), 926.60 (50.30), 890.60 (54.38), 815.60 (36.47), 785.60 (34.07), 752.60 (47.09), 727.65 (66.60), 671.70 (38.21), 668.70 (39.81), 638.70 (36.81), 591.65 (72.48), 543.30 (48.90), 517.75 (54.24), 468.35 (87.51), 432.55 (74.22), 368.95 (67.94), 363.50 (51.70), 335.10 (51.37), 310.10 (36.94), 296.10 (61.06), 255 (46.36), 253 (45.29), 226 (50.70), 222.40 (76.49), 210.35 (75.28), 195 (39.08), 183 (59.39), 162.80 (56.78), 153.30 (38.41), 139.15 (35.14), 133.20 (19.44), 123.70 (51.90), 121.60 (52.10), 107 (16.43), 96.20 (50.30), 87.50 (83.97), 82.55 (56.51), 81.55 (31.26), 66.10 (81.43), 64 (100).

Table 5. Thermal analysis data for 2'-hydroxychalcone and its complexes.

Comp. No.	Molecular formula	Molecular weight	Decomposition step (K)	T_g	Weight loss (%) (Found)	Weight loss (Calc)	Eliminated species	Solid residue, (%)
1	ChOH	284.31	467-573	555.97	100%	284	--------	------
2	$[Cr_2O_2 (ChO)_2]$	702.59	333-467	420.76	18.72	19.44	$C_8H_9O_2$	23.48 (21.57)
			468-723	657.14	56.66	(53.36)	$L + C_6H_4O$	(Cr_2O_3)
3	$[Mo_2O_4 (ChO)_2]$	822.48	333-773	709	32.36	32.52	$C_{17}H_{16}O_2$	31 (29.13)
			883-1123	1049.57	40.12	38.30	$C_{17}H_{16}O_4 + O_2$	Mo_2O_3
4	$[W_2O_4 (ChO)_2]$	998.30	333-478	410.05	22.92	25.22	$C_{17}H_{16}O_2$	46.33 (44.40)
			457-1103	554.87,			$C_{17}H_{16}O_4 + O_2$	2 WO2
				899.94	30.63	31.66		
5	$[Ru_3(CO)_{10-}(ChO)$	866.61	333-458	449.65	32.73	32.33	10 CO	34.86 (34.99)
			459—798	519.12	32.41	32.68	$C_{17}H_{16}O_4$	3 Ru
6	$[Os_3(CO)_{10-}(ChOH)]$	1135.10	313-483	452.37	25.44	24.66	10 CO	----
			484-643	558.92	25.61	25.0	$C_{17}H_{16}O_4$	
			644-1003	771.9	49.25	50.22	3 Os	

Table 6. The inhibition zones (mm) of ChOH and its complexes. The activity of 2.5mg/ml of the sample, Amikacin was used as standard.

Comp. No.	M. Formula	*B. subtillus*	*S. aureus*	*E. coli*	*P. aeruginosa*	*C. albicans*
2	$[Cr_2O_2 (ChO)_2]$	22	19	25	17.5	20
3	$[Mo_2O_4 (ChO)_2]$	19	20	21	18	18.5
4	$[W_2O_4 (ChO)_2]$	20	19	20	20	20
5	$[Ru_3(CO)_{10}(ChO)$	22	20	21	23.5	23
6	$[Os_3(CO)_{10}(ChOH)]$	22	20	20	22	20
1	ChOH	20	19	17	20	21
	Amikacin	29	31	34	32	25

Table 7. Minimum Inhibitory Concentration (M.I.C) of ChOH and its complexes against microorganisms. Amikacin was used as standard.

Comp. No.	M. Formula	*B. subtillus*	*S. aureus*	*E. coli*	*P. aeruginosa*	*C. albicans*
2	$[Cr_2O_2 (ChO)_2]$	156	312	625	1250	625
3	$[Mo_2O_4 (ChO)_2]$	312	312	625	1250	1250
4	$[W_2O_4 (ChO)_2]$	312	312	312	625	312
5	$[Ru_3(CO)_{10}(ChO)$	312	312	625	625	312
6	$[Os_3(CO)_{10}(ChOH)]$	156	312	625	312	625
1	Ch-OH	312	312	625	312	625
	Amikacin	19.53	19.53	9.76	9.76	39.06
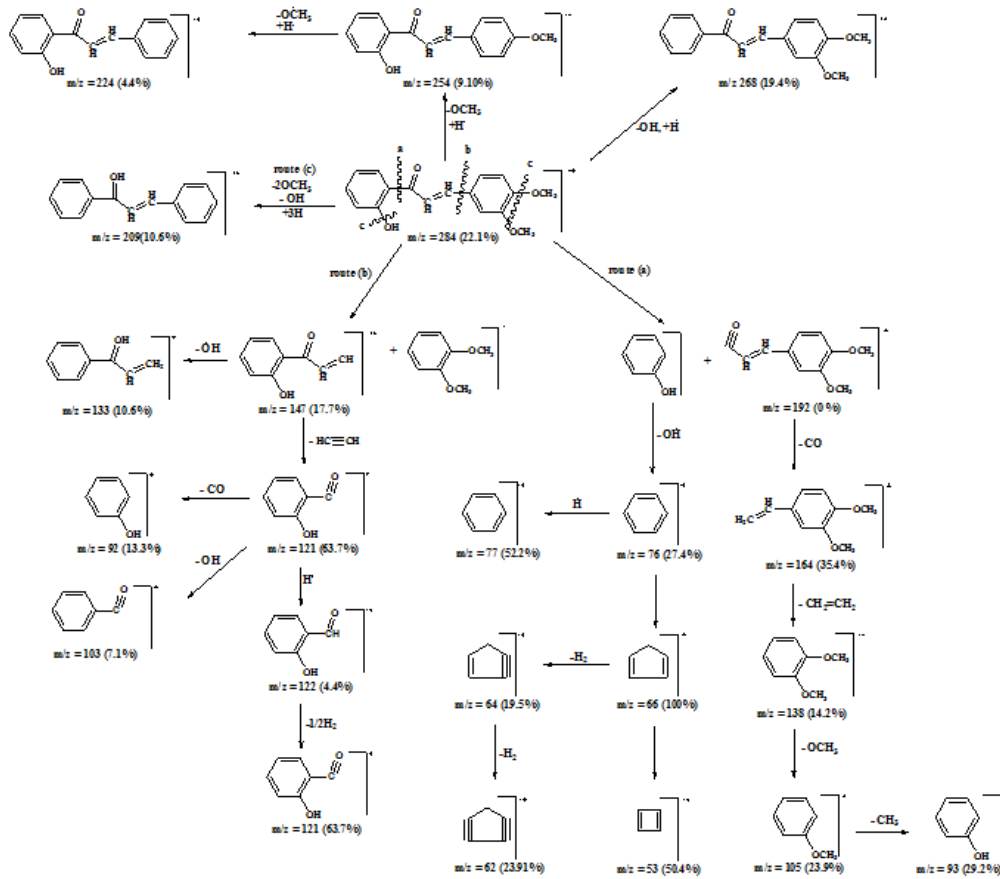
Chart No. 1

EI-fragmentation pattern of compound 1
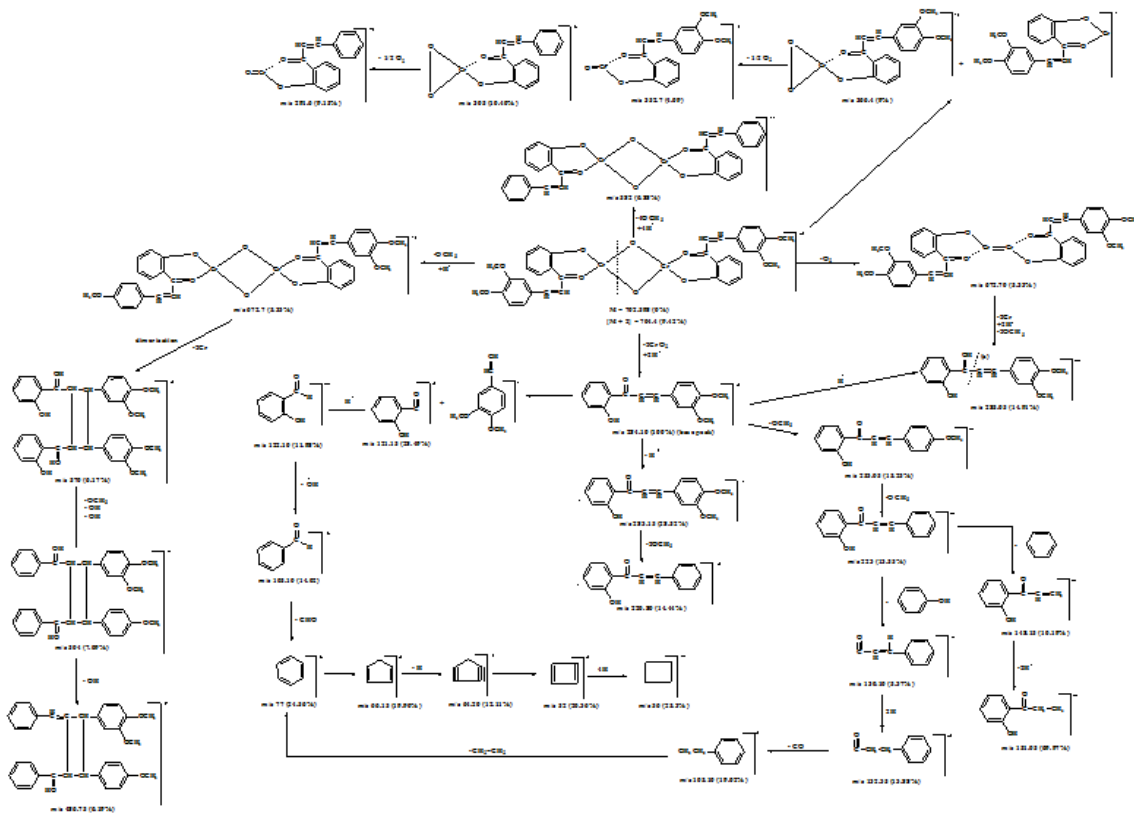
Chart No.2

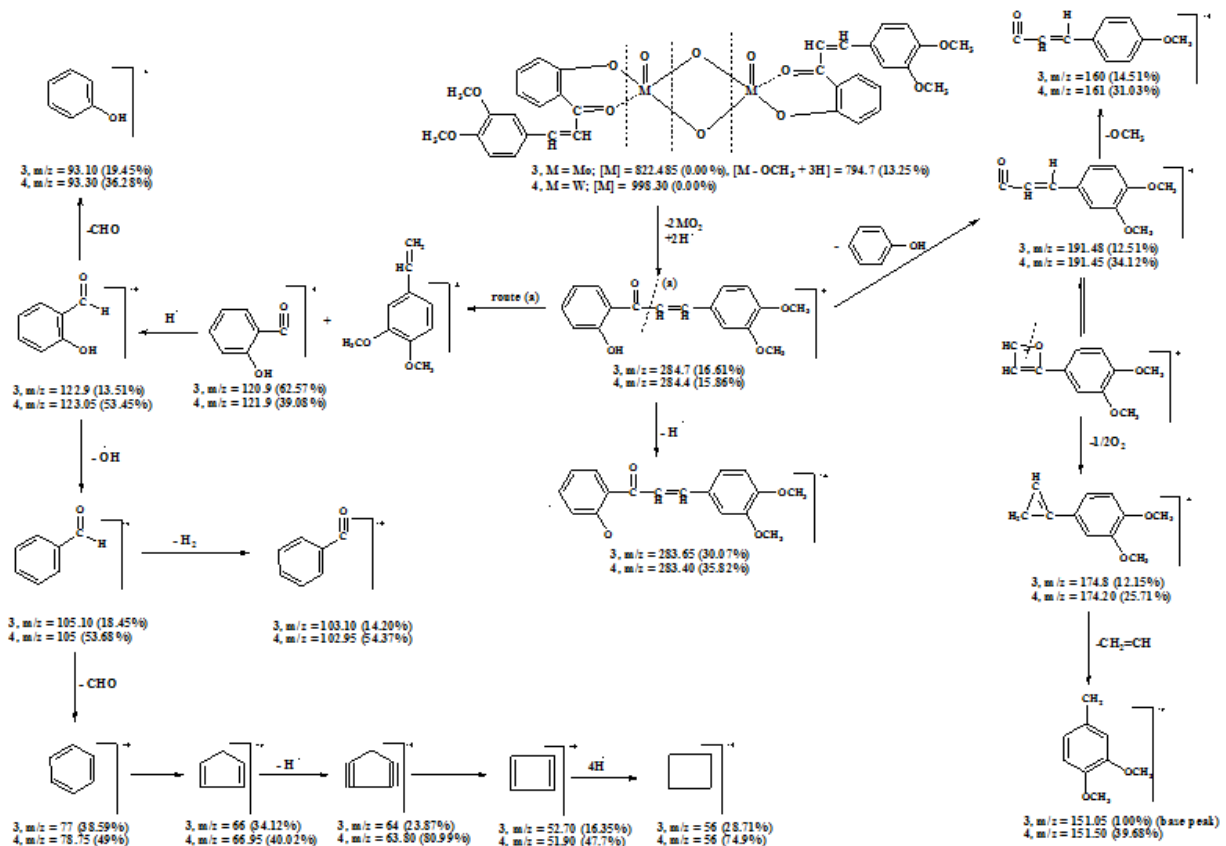**EI-fragmentation pattern of compound 2**

Chart No. 3
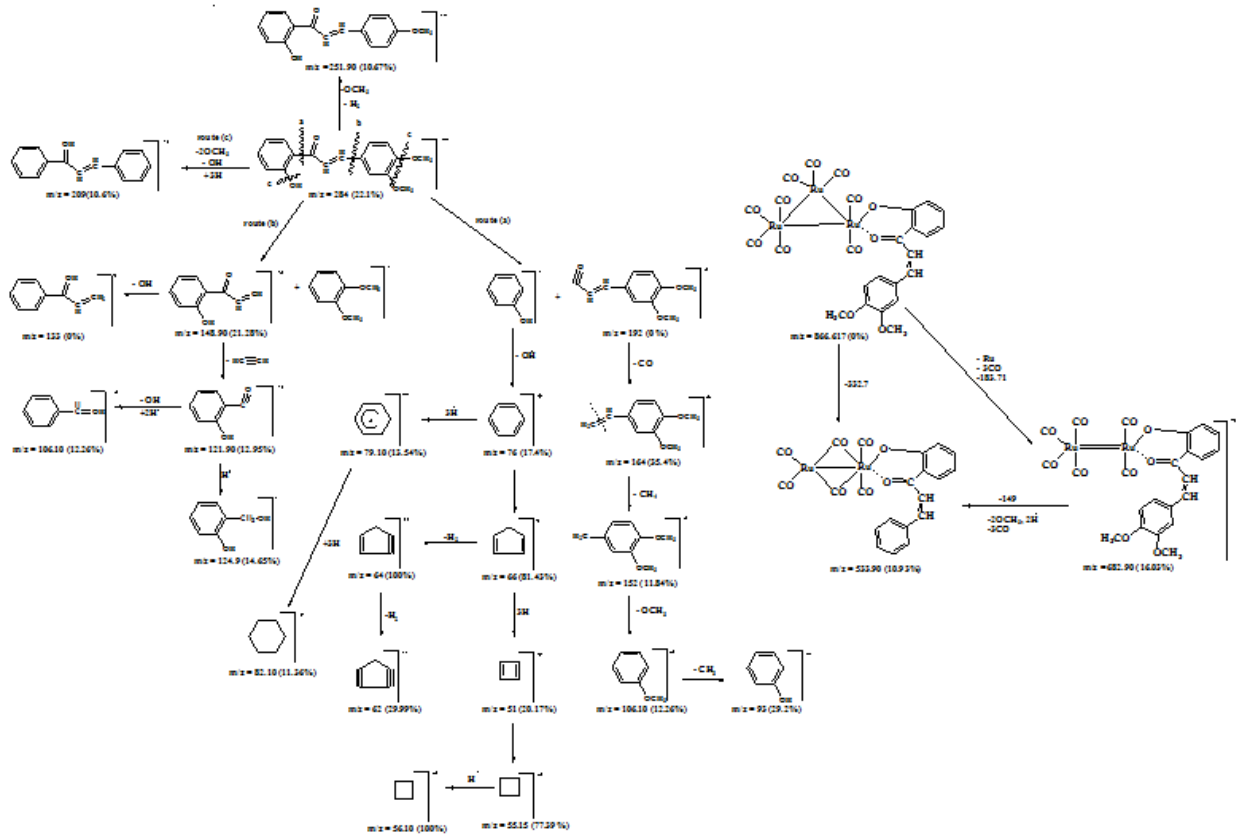**EI-fragmentation pattern of compounds 3 & 4**

Chart No. 4
EI-fragmentation pattern of compound 5

References

1) R.S. Naidu, E.N. Rao, R. Ruby and K. Mallikarjun (1988). Thermchim. Acta 131: 299.

2) a) N.B. Pappano, O.P. Centrobi, F.H. Ferretti (1994). Rev. Microbiol. Sao Paulo 25: 305.
   b) Vyas K.B., Ninavat K.S., Jani G.R., Hathi M.V. (2009). Orbital, 1: 1837.

3) S.D. Lorimer, N.B. Perry (1994). Planta. Med 60: 386.
   b) RS Naidu, EN Rao, R. Ruby, K. Mallikarjun (1989). Thermchim. Acta 140: 97.

4) M. I. El-Gamal, S. M. Bayomi, S. M. El-Ashry, S. A. Said, A. A.-M. Abdel-Aziz, N. I. Abdel-Aziz (2010). Eur. J. Medici. Chem., 45: 1403.

5) R. G. Damazio, A. P. Zanatta, L.H.Cazarolli, L.D.Chiaradia, A.Mascarello, R.J. Nunes, R.A. Yunes, F. Regina, M. Barreto Silva (2010). *Eur.J. Medicin.Chem.*, 45: 1332.

6) V.S. Parmar, R. Jain, K.S. Sharma,, A. Jha, P. Taneja, S. Singh., M.B. Vyncke, M.E. Bracke, M.M. Marcel (1994). J. Pharma. Sci. 83: 1217.

7) H.-Yao Tu, A-Mei Huang, Tzyh-Chyuan Hour, Shyh-Chyun Yang, Yeong-Shiau Pu, Chun-Nan Lin (2010). *Bioorg Med. Chem. 18*: 2089.

8) X. Chen, Li-Jun Tang, Yu-Na Sun, Pei-Hong Qiu, Guang Liang (2010). J. Inorg. Biochem., 104: 379–384.

9) R.J. Anto, Sugumaran, G. Kuttan, MNA Rao, V. Subbaraju, R Kuttan (1995). Cancer Lett. 97: 33.

10) C.X. Xue, S Y. Cui, M.C. Liu, Z D. Hu, B.T. Fan (2004). Eur. J. Med. Chem. 39: 745.

11) O. Sabzevari, G. Galati, , M.Y. Mordani, A. Siraki, P.J. O'Brein (2004). Chem. Biol. Interact 148: 57.

12) Z. Rozmer, T. Berki, P. Perjési (2006). Toxicol. Vitro 20: 1354–1362.

13) B. M. Rezk; G. R. M. M. Haenen; W. F. F. Van der Vijgh; A. Bast (2002). Biochim. Biophys. Res. Commun., 295: 9.

14) L. Mishra, R. Sinha, H. Itokawa, K.F. Bastow, Y. Tachibana, Y. Nakanishi, N. Kilgore, K.H. Lee (2001). Bioorg. Med. Chem. 9: 1667

15) L. Mishra; R. Sinha (**2000**). *Indian J. Chem., Sec. A*, 39A: 1131.

16) H. Wang, Y. Wang, Z.Y. Chen, F.L. Chan, L.K. Leung (2005). *Toxocology* 207: 303.

17) M. Palaniandavar, C. Natarjan (1980). Aust. J. Chem. 33: 737.

18) T.S. Rao, K.L. Reddy, P. Lingaiah (1988). Indian J. Chem. 27A: 510.

19) S. Arvindakshan, K.K. Polyhedron (1993) 12: 1187.

20) M.V. Kaveri, R. Prabhakaran, R. Karvembu, K. Natarajan (2005). Spectrochim. Acta A 61: 2915.

21) M. Muthukumar, P. Viswanathamurthi (2009). Spectrochimica Acta A 74: 454.

22) R. Prajapati a, S. K. Dubey, R. Gaur, R. K. Koiri, B. K. Maurya, S. K. Trigun, L. Mishra (2010). Polyhedron 29: 1055–1061.

23) A.M. Brodie, B.F.G. Johnson, P.L. Josty, J. Lewis (1972). J. Chem. Soc., Dalton. Trans., 2031.

24) K. Zutin, V.M. Nogueira, A.E. Mauro, P. Melnikov, A. Iluykhin (2001). Polyhedron 20: 1011–1016.

25) R.E. Cooper (1972). "Analytical Microbiology" F.W. Kavanageh (ed), Vol I & II Academic Press, New York and London.

26) S. Mackay, C.J. Gilmore, C. Edwards, N. Stewart, K. Shankland (1999). maXus Computer Program for the Solution and Refinement of Crystal Structures. Bruker Nonius, The Netherlands, Mac-Science, Japan, and The University of Glasgow.

27) A. Altomare, G. Cascarano, C. Giacovazzo, A. Guagliardi, M.C. Burla, , G. Polidori, M. Camalli (1994). J. Appl. Cryst. 27: 435.

28) C.K. Johnson (1976). ORTEP–II. A Fortran Thermal–Ellipsoid Plot Program, Report ORNL-5138. Oak Ridge National Laboratory, Oak Ridge, Tennessee, USA.

29) T. Szymańska-Buzar (2006). Coordination Chemistry Reviews 250: 976–990.

30) O. S. Senturk; U. Ozdemir; S. Sert;, N. Karacan; F. Ugur (2003). Inorg. Chem. Commun. 6: 926.

31) E. Subasi;, O. S. Senturk;, F. Ugur (2004). Trans. Met. Chem. 16: 29.

32) M. J. Almond, F. Sarıkahya, O. S. Senturk (1997). Polyhedron 16: 1101.

33) S. Sert, O. S. Senturk, F. Sarıkahya (2003). Tran. Met. Chem. 28: 133.

34) M. M. H. Khalil, F.A. Al-Seif (1997). J. Coord. Chem. 60X: 1191.

35) F.A. Cotton, G. Wilkinson, C.A. Murillo, M. Bochmann (1999). *Advanced Inorganic Chemistry*, John Wiley, New York.

36) C.G. Pierpont (2001). Coord. Chem. Rev. 415: 219.

37) R.M. Ramadan, M.S.A. Hamza, S.A. Ali (1998). J. Coord.Chem. 43: 31.

38) S.A. Ali, M.M.H. Khalil, R.M. Ramadan (2000). Trans. Met. Chem., 25: 121.

39) R.S. Drago (1986). *Physical Methods in Chemistry*, Saunders, Philadelphia.

40) H. Aritani, O. Fukuda, A. Miyaji, S. Hasegawa (2001). Appl. Surface Sci. 180: 261-269.

41) D.Y. Sabry, T.A. Youssef, S.M. El-Medani, R.M. Ramadan (2003). J. Coord. Chem. 56: 1375.

42) O.A.M. Ali, M.M.H. Khalil, G.M. Attia, R.M. Ramadan (2003). Spectroscopy Lett. 36: 71.